Aquaculture International (2024) 32:1427–1451
https://doi.org/10.1007/s10499-023-01223-3

Molecular characterization of *Rab5A*, and involvement in innate immunity in Yellow River Carp *Cyprinus carpio*

Guilan Di[1,2] · Zeyuan Ma[1] · Mingmei Jiang[1] · Yu Zhang[1] · Ning Wang[2] · Xinhua Chen[1,3]

Received: 14 June 2023 / Accepted: 25 July 2023 / Published online: 30 August 2023

Abstract
Rab5A play important roles in regulating trafficking organelles, especially in phagosome formation. In the present study, full-length cDNA sequences of Rab5A were cloned from Yellow River Carp *Cyprinus carpio*, which was designated as *Cc*Rab5A. The full-length cDNA of the *Cc*Rab5A cDNA sequence is 2434 bp and included an open reading frame (ORF) encoding 216 amino acids polypeptide with an estimated molecular weight of 23.47 kDa. Bioinformatics analysis showed that the *Cc*Rab5A protein was highly conserved during evolution. *Cc*Rab5A's deduced amino acid sequence showed high identity to *Cyprinus carpio* (99.54%) in comparison. The guanine-base binding motif (G), phosphate/magnesium-binding motif (PM), and Rab family motif (Rab F) of *Cc*Rab5A are highly conserved among various species, but the N- and C-terminal regions were hypervariable, according to the results of multiple sequence alignment and phylogenetic analysis. Additionally, 11 tissues of Yellow River Carp were examined using Real-time Fluorescence Quantitative PCR (qRT-PCR) to determine the expression levels, with the highest expression levels in head kidney and blood. Followed by heart, liver, muscle, brain, gill, skin, spleen and intestine; The expression level in body kidney was the lowest. Yellow River Carp was immunized with *Aeromonas hydrophila* and Spring viremia of carp virus (SVCV) respectively, and the expression changes of *Cc*Rab5A in gill, spleen, liver, intestine and skin of Yellow River Carp were detected. The results showed that the expression level of the gene was obviously up-regulated at different time points. The eukaryotic recombinant plasmids of *Cc*Rab5A, pEGFP-N3 were constructed and transfected into GCO cells for subcellular localization. The results showed that *Cc*Rab5A were mainly distributed in nuclear membrane and various endosome membranes. These results showed that *Cc*Rab5 were involved in viral and bacterial infection in the immune response of Yellow River Carp.

Handling Editor: Brian Austin

Guilan Di and Zeyuan Ma contributed equally to this work.

A Rab5A homologue protein (*Cc*Rab5A) was identified from Yellow River Carp *Cyprinus carpio*.

✉ Ning Wang
wangningscxy@163.com

✉ Xinhua Chen
chenxinhua@tio.org.cn

Extended author information available on the last page of the article

Keywords Yellow River Carp *Cyprinus carpio* · *CcRab5A* · Molecular characterization · Immune function

Introduction

Small G protein plays an important role in the downstream signaling of various plasma membrane receptors. Ras-associated binding (Rab) proteins are the most numerous branch of the Ras-like small GTPase superfamily, with over 70 Rab proteins identified to date (Li and Marlin 2015). To perform its physiological functions, Rab protein switches pathways by regulating the GTP-GDP cycles. The activated state of GTP binding is generally found in the cell membrane, whereas the inactive state of GDP binding is found throughout the cytoplasm. The various components are located at both ends of the peptide segment. The protein's binding to a specific membrane vesicle is determined by the 35 amino acids at the C terminal, while its binding to the N terminal is determined by the 20 amino acids with a specific receptor membrane. Rab protein family members are high conservation of phosphate/magnesium-binding (PM) motifs, guanine-base binding (G) motifs, and Rab family motifs (RabF) of Rab proteins across different species (Pereira-Leal and Seabra 2001; Valencia et al. 1991; Flannagan et al. 2012).

Rab proteins are key regulators of the endocytic pathway (Hutagalung and Novick 2011). Rab protein regulates endosomes and lysosomes and participates in endocytosis (Lund et al. 2018). Rab5 is one of the most important members of the Rab family, acting as a regulator in the fusion of endosome and phagosome in early process of phagocytosis and endocytosis, and mediates traffic from the plasma membrane to the early endosomes, as well as acting as an early endosome marker (Bucci et al. 1992). Rab5 gene expression is ubiquitous in various tissues, Rab5a, Rab5b, and Rab5c are three isoforms of Rab5 found in mammalian cells, and their cellular localization is overlapping and functionally related (Bucci et al. 1995). Mammalian Rab5, for example, associates with early endosomes (EE) and is a key rate-limiting component of the EE pathway (Barbieri et al. 2000). Rab5 controls cargo entry from the plasma membrane to the EE (Murray et al. 2002). During the phagocytosis process, it was discovered that Rab5 was rapidly enriched on early phagosomes of human macrophages. After cytosolic Rab5 immunodepletion, the fusion of the phagosome and the endosome was significantly reduced, and Rab5 overexpression could improve the fusion of the phagosome and the lysosome (Alvarez-Dominguez et al. 1996; Alvarez-Dominguez and Stahl 1999). Additionally, phagocytic capacity was impacted by the loss of Rab5 (Bucci et al. 1992), Rab5 works with its effector molecules to contribute to the development of the cytoskeleton without the assistance of PI3-K, Rac, Ras, and Cdc42. Rab5 could lead to the reorganization of the actin cytoskeleton, Lamellipodia will form and cells will migrate as a result of Rab5-regulated cytoskeletal structure changes, which may help and direct cytophagocytosis (Spaargaren and Bos 1999). Rab5 expression changes are linked to a variety of diseases. Rab5 mutations have been linked to neurological and immune system diseases (Li and Marlin 2015).

In innate immunity, the Rab protein is important in pathogen scavenging by phagocytic cells (Galea et al. 2015). Recent research suggests that Rab may be involved in host cell defense against pathogen infection (Ye et al. 2012). According to recent studies (Han et al. 2017; Liu et al. 2018), Rab5 is also implicated in aquatic species' innate immunity. In the spleen of giant yellow croakers *(Larimichthys crocea*) infected with *Vibrio parahaemolyticus*, Rab5 mRNA expression was dramatically enhanced (24.1 times compared to the control). Additionally, through promoting the production of IL-6 and TNF, Rab5 overexpression may enhance the giant yellow croaker's inflammatory response (Han et al. 2017). White spot syndrome virus

(WSSV) and infectious hypodermal and hematopoietic necrosis virus (IHHNV) infections drastically changed the expression of the Rab5 gene in *Litopenaeus vannamei*, and Rab5 was also able to interact with IHHNV's non-structural protein NS1 (Liu et al. 2018).

As one of the important economic fish, Yellow River Carp (*Cyprinus carpio* L.) are widely cultivated in aquaculture along the Yellow River in China. However, Yellow River Carp have recently been plagued by a variety of bacterial and viral illnesses, resulting in large economic losses. As a result, it is critical and urgent to effectively control the disease outbreak in Yellow River Carp. Spring Viraemia of Carp Virus (SVCV) and *Aeromonas hydrophila* were both serious threats to *C. carpio* culture (Qiao et al. 2023; Li et al. 2023). Despite significant progress in understanding the virus's infection mechanism, there was no effective method for controlling *C. carpio* SVCV disease. *C. carpio* was also susceptible to Spring Viraemia of Carp Virus (SVCV) infection, which posed a serious threat to *C. carpio* culture, particularly in China (Ashraf et al. 2016). According to several studies (Santos et al. 1987; Liu et al. 2007; Baumgartner et al. 2009), *A. hydrophila* was a prevalent and ubiquitous pathogenic bacteria in aquatic ecosystems that could infect a variety of aquatic creatures, including fish, shrimp, and crayfish. As a result, it is now of utmost importance to do study on *Cyprinus carpio*'s immunological function. There haven't been many investigations on the immunological and structural properties of *Cc*Rab5A from fish, notably *C. carpio*. The current work aims to look into the molecular properties and tissue distribution of CcRab5A from *C. carpio*, as well as its immunological function against several pathogens (SVCV and *A. hydrophila*). The findings of this investigation may offer crucial evidence in favor of future research on the immunological function of Rab proteins in Yellow River Carp.

Materials and methods

Experimental animals

Yellow River Carp *C. carpio* individuals (weighing approximately 30 ± 5 g) were collected from a local farm in Xinxiang, Henan Province, China. They were kept in 200 L tanks for seven days prior to the experiment at Henan Normal University. The fish were randomly separated into 3 groups with 30 fish in each group. Each tank held 100 L of aerated water, and the fish were fed with pellets at 5% body weight. Every three days, one-third of the water was changed. The water temperature was kept at 25 ± 2 °C, and pH was kept at 7.0 ± 0.2. All animal experiments in this study were carried out in accordance with the protocols of the Ministry of Science and Technology's "Guidelines for Experimental Animals" (Beijing, China), and all experiments were carried out in accordance with the animal ethics guidelines approved by the Henan Normal University's Ethics Committee.

Bacterial strain

A. hydrophila was identified from sick commercially farmed carp with spontaneously occurring bacterial enteritis and collected from Xinxiang, China in 2016. The bacteria were then identified as *A. hydrophila* using established biochemical diagnostic procedures (Di et al. 2017). In terms of bacterial stimulation, a single colony was injected into LB and cultured at 28 °C for 16 h. Centrifugation at 3500 rpm for 5 min yielded *A. hydrophila*, which was washed in physiological saline solution (PSS). Bacterial concentration was measured in colony forming units (CFU) per mL by plating tenfold

successive dilutions of 10 mL onto LB agar plates. After then, the cells were suspended in PSS. *Aeromonas hydrophila* challenge procedures are similar to those previously reported (Di et al. 2017). Fish in the *A. hydrophila* stimulated group were intraperitoneally injected with 100 µL bacteria at a concentration of 5×10^6 CFU/mL, whereas the control group received the same volume of PBS (Di et al. 2017).

Cell line and SVCV propagation

Epithelioma papulosum cyprinid (EPC) cells were cultivated at 28 °C in Leibovitz's L-15 medium (Gibco, USA) supplemented with 10% fetal bovine serum (FBS; Gibco) at 28 °C. The grass carp ovary cell line (GCO cells) was kindly provided by Institute of Hydrobiology, Chinese Academy of Sciences, GCO cells were routinely grown in M199 medium (Hyclone, USA), supplemented with 10% fetal bovine serum (FBS, Gibco, USA), and penicillin–streptomycin (1%) mixture with a 5% CO_2 at 26 °C.

For the SVCV challenge, the virus strain was isolated from common carp (Chen et al. 2006), SVCV was kept in our laboratory and propagated in EPC cells supplemented with 10% fetal bovine serum (FBS, Gibco, Thermo Fisher) at 25 °C until a terminal cytopathic effect (CPE) developed (Li et al. 2023). Following that, the harvested SVCV was kept at 80 °C for future use. Virus titers were assessed using the prior approach (Chen et al. 2022). To summarize, the virus was serially diluted ten times and 100 µL of each dilution was added to eight wells. Under an inverted microscope, the cytopathic effects (CPE) were continually detected in infected cells for 96 h. Furthermore, to visualize CPE, the cell monolayers were fixed with 4% paraformaldehyde and stained with 1% crystal violet (Beyotime, China). The viral titer with 50% tissue culture infective dose ($TCID_{50}$) analysis was performed using the Reed-Muench technique in cell-cultured 96-well plate for 48 h post-infection (hpi). EPC cells were treated with SVCV at $10^3 \times TCID_{50}$ for viral infection in vitro. After 1 h, the supernatants were changed, and the cells were washed three times with cell medium before being incubated in M199 medium containing 5% FBS at 25 °C. Before exposing the fish to SVCV, reverse transcription polymerase chain reaction (RT-PCR) and nested PCR utilizing SVCV-specific primers targeting the glycoprotein (G) gene were performed (Kim 2012). Yellow River Carp were intraperitoneally injected with 100 µL of SVCV (1×10^5 $TCID_{50}$/ mL) for viral infection, whereas Yellow River Carp were treated identically and intraperitoneally injected with 10 µL of PBS as the control group.

RNA extraction and cDNA preparation

Total RNA was extracted from Yellow River Carp *C. carpio* tissue using RNAiso Plus. The concentration of RNA was determined using a NanoDrop 2000 spectrophotometer (Thermo Scientific, USA), and the RNA integrity was determined using electrophoresis on a 1.0% agarose gel. The first strand of cDNA was synthesized using the PrimeScriptTMII1st Strand cDNA Synthesis Kit and oligo dT-adaptor as primers, following the manufacturer's protocol (TaKaRa, China). The synthesis reaction was carried out at 42 °C for 1 h before being stopped by 5 min of heating at 95 °C. The cDNA mixture was diluted 1:40 and kept at -80 °C.

Gene amplification of *Cc*Rab5A in Yellow River Carp

To amplify the corresponding core cDNA sequences, *Cc*Rab5A degenerate primers were made utilizing conservative amino acids (Table 1). A total of 20 μL of mixture, consisting of 1 μL of cDNA template, 1 μL of each primer, 10 μL of Taq Master Mix (Taq DNA Polymerase, PCR Buffer, Mg2+, dNTPs), and 7 μL double-distilled water (ddH2O), was produced for PCR reactions. The PCR conditions were as follows: a 5-min predenaturation at 94 °C, 34 cycles of 30 s of denaturation at 94 °C, 30 s of annealing at 60 °C, 45 s of extension at 72 °C, and 10 min of final extension at 72 °C. The core sequence of CcRab5A was used to create the RACE primers (Table 1). The rapid amplification of cDNA ends (RACE) technique was then used to extract the 3′ and 5′ end sequences of CcRab5A, respectively.

The PCR products were purified using an Agarose Gel DNA Purification Kit (TaKaRa, Japan) after being collected on a 1.0% agarose gel. The purified DNA fragments were then transferred into *E. coli* DH5 cells using the pMD19-T vector (TaKaRa, Japan) and cloned. Sequencing was done on colonies that were positive. The CDS sequences of the *Cc*Rab5A were verified by PCR. Table 1 contains a list of the primers utilized in this investigation.

Sequence analysis and phylogenetic tree construction

The nucleotide sequence was translated using the ExPASy Translate tool (http://web.expasy.org/translate/), and the resulting protein sequences were compared to other sequences in the NCBI database using the online search tool BLASTX (http://www.ncbi.nlm.nih.gov/). The BLAST tool (http://blast.ncbi.nlm.nih.gov/Blast.cgi) was used to perform homologous analysis on the cDNA sequences and amino acid sequences of CcRab5A from the National Center for Biotechnology Information (NCBI) database. the NCBI ORF finder (http://www.ncbi.nlm.nih.gov/gorf/gorf.html) was used to identify the open reading frames (ORFs). The ExPASy Compute pI/Mw tool (http://web.expasy.org/compute pi/) was used to calculate the isoelectric point and molecular weight. To predict the presence of signal peptides, the Signal P 4.1 Server (http://www.cbs.dtu.dk/services/SignalP/) was used, and SMART (http://smart.emblheidelberg.de/) was used to predict domain structure and function. To predict transmembrane regions, TMHMM Server v.2.0 (http://www.cbs.dtu.dk/services/TMHMM/) was used. DNAman software was used to align nucleic acid and amino acid sequences. PSIPRED (http://bioinf.cs.ucl.ac.uk/psipred/) and SWISS-MODEL (http://swissmodel.expasy.org/) were used as online software, *Cc*Rab5A three-dimensional models were built. ClustalX 2.0 and DNAMAN software were used to perform multiple sequence alignment of *Cc*Rab5A. MEGA 7.0 software was used to create phylogenetic trees using the neighbor-joining (NJ) method. The amino acid sequences of *Cc*Rab5A from various species were searched for multiple sequence alignment and phylogenetic analysis using the BLASTp program in the NCBI server (http://blast.ncbi.nlm.nih.gov/Blast.cgi) and NCBI GenBank (http://www.ncbi.nlm.nih.gov/genbank/).

Tissue distributions of *Cc*Rab5A

Eleven carp tissues were collected from five healthy Yellow River Carp *C. carpio*, including the head kidney, blood, liver, heart, muscle, intestine, spleen, gill, brain,

Table 1 Sequences of the primers used in this study

Gene	Primer name	Primer Sequence (5′-3′)	Usage
	Clone primers		
	RAB5A-F	AGGAAAGCACAATAGGAGCG	Intermediate fragment primer
	RAB5A-R	AGTGCGAGCGTGACTGGTGC	
	RAB5A-3'-Out	CATGCCGTGTCTCCGAATTG	3'RACE
	RAB5A-3'-In	GGTTCACCTGCCCTGTCATA	
	RAB5A-5'-Out	TTGGACTGGCCTGCCTCTG	5' RACE
	RAB5A-5'-In	AATGGCAGCCTGGGCACCT	
	3' RACE Olig(T)-Adaptor	CTGATCTAGAGGTACCGGATCC$(T)_{14}$	Adaptor Primer for RACE
	3' RACE Adaptor	CTGATCTAGAGGTACCGGATCC	
	5' RACE Olig(T)-Adaptor	GACTCGAGTCGACATCGA$(T)_{17}$	
	5' RACE Adaptor	GACTCGAGTCGACATCG	
	Recombinant expression		
	RAB5A-F1	CGGGATCCATGGCCAATAGGGGAGGAGC	
	RAB5A-R1	CCCAAGCTTGGTTGCTGCAGCAGGGGGC	
	RT-PCR primers		
Rab5A	QRab5A-F	TTGTCATCGCACTGTCTGGG	RT-PCR
	QRab5A-R	GGGCTCATTCTTAGGCAACC	
β-actin	βCCF	TGCAAAGCCGGATTCGCTGG	
	βCCR	AGTTGGTGACAATACCGTGC	
	Eukaryotic expression primers		
Rab5A	NRab5AF	CCCAAGCTTCGATGGCCAATAGGGGAGGAGC	
	NRab5AR	CGGGATCCGTTGCTGCAGCAGGGGGC	
pEGFP-N3	N3F	TGGGAGGTCTATATAAGCAGAG	
	N3R	CGTCGCCGTCCAGCTCGACCAG	

The underlined part of the primer sequences represent the restriction sites

skin, and kidney, to investigate *Cc*Rab5 tissue expression using quantitative real-time RT-PCR on a 7500 Real-time Fluorescent Quantitative Instruments. RNA extraction and first-strand cDNA synthesis were carried out. The primers (Table 1) were used to amplify *Cc*Rab5A. According to the previous study, the 18S rRNA primers were used to amplify the internal control 18S rRNA (Qin et al. 2019). In a total volume of 20 μL, the qRT-PCR reaction mixture included specific primer (10 mM), SYBR Premix Ex Taq TMII (TaKaRa, Japan), and cDNA template. The PCR reactions were carried out after 95 °C for 1 min, followed by 40 cycles of 95 °C for 10 s, 60 °C for 30 s, and 72 °C for 20 s. The 2-ΔΔCt method was used to calculate the relative expressions of *Cc*Rab5A.

Tissue distribution and expression profiles of *Cc*Rab5A after pathogen infection

Yellow River Carp were divided into three groups: two experimental groups (SVCV and *A. hydrophila* infected groups) and a control group, 72 fish in each of the three groups, each group of 72 fish was carried out in triplicate. Each carp in the *A. hydrophila*-infected group received a 100 μL live *A. hydrophila* suspension injection (approximately 5×10^6 CFU mL^{-1}). Each carp in the SVCV-infected group received a 100 μL injection of SVCV at a copy number of 10^5/mL. As a control, carps were given an injection of 100 μL of sterile physiological saline solution. Following injection, the carps were returned to their water tanks, and nine individuals from each group were chosen at random and separated into three groups for tissue collection at 0, 6, 12, 24, 48, and 72 h after injection (hpi). Three fish were randomly selected from each group (three from each replicate). For subsequent RNA extraction, all of these samples were stored at -80 °C with Trizol reagent. The fish's intestinal tract, liver, gills, skin, and spleen were then sampled. Then, using the methods described above, qRT-PCR was performed on each sample in triplicate.

Recombinant expression and purification of recombinant proteins

The open reading frame (ORF) sequence of *Cc*Rab5A was amplified using the primers *Cc*Rab5A -F and *Cc*Rab5A-R (Table 1). The PCR products were digested with BamH I and Hind III before being transformed into Escherichia coli BL21 (DE3) cells with the recombinant expression plasmid pET-32a-*Cc*Rab5A The positive clone was confirmed by PCR and inoculated into ampicillin-containing LB medium. Following induction with IPTG, the fusion protein was purified using a Ni2 + -chelating Sepharose column (Sangon Biotech, China) for the following far western blotting assay.

Preparation of polyclonal antibody against *Cc*Rab5A and western blot analysis

Using the BCA Protein experiment Kit in a Western blot experiment (Beyotime Biotechnology, Shanghai, China), protein was extracted from diverse tissues and measured. 12% SDS-PAGE was used to separate the protein. After that, the SDS-PAGE gel was transferred to the nitrocellulose membrane. The nitrocellulose membrane was cleaned before being blocked with a solution that contains 5% skim milk for an hour. A mouse anti-Rab5A antibody was added after the membrane had undergone three washings. Goat anti-mouse antibody that had been HRP-labeled was incubated for two hours at room temperature after being incubated overnight at 4 °C. The membrane was detected using an enhanced chemiluminescence system after being washed three times (ECL).

Construction of eukaryotic plasmid

Based on the coding sequence of the *Cc*Rab5A gene, forward primer Rab5A-F (5'-CCCAAGCTTCGATGGCCAATAGGGGAGGAGC-3', the underlined letters indicated BamHI restriction enzyme site) and reverse primer (5'-CGGGATCCGTTGCTGCA GCAGGGGGC-3', Hind III restriction enzyme site was indicated by the underlined letters) were created. Following that, the PCR reactions were carried out, and the results were acquired via the aforementioned techniques. Following that, BamHI and Hind III restriction enzymes were used to digest the PCR products and pEGFP-N3 vectors, and after that, T4 DNA ligase overnight ligated them. The target gene was confirmed by sequencing the associated products after they had been transformed into *E. coli* strain DH5.

Cell transfection

The recombinant plasmids were transfected into GCO cells, which were then grown for 24 h to achieve roughly 80% confluence before being transiently transfected with the indicated plasmids using Lipofectamine 2000 reagent (Invitrogen, USA) according to the manufacturer's procedure. To summarize, 6 μg of each plasmid and 10 μL of Lipofectamine were diluted in 250 μL of serum-free medium containing M199 (Hyclone, USA), with the pEGFP-N3 plasmid serving as a control. After 20 min, the mixture was applied to the cells and incubated for 6 h at 28 °C. Cells were grown at 28 °C for 48 h post transfection after being replaced with serum-containing medium.

Subcellular localization of *Cc*Rab5A

Extracted recombinant plasmid, grass carp ovary cell lines (GCO), were used in the study. GCO cells were seeded into a 6-well plate, recombinant plasmid/pEGFP-N3 was added to the 6-well plate, fixed with 4% para-formaldehyde solution for 15 min at room temperature, treated with 1 mL 0.2% TritonX-100 for 15 min at room temperature, and cells were then Fluorescence microscopy allowed for the observation of subcellular localization.

Statistical analysis

Using IBM SPSS Statistics 19's one-way analysis of variance (ANOVA), the statistical significance was established. The significance and extremely significant thresholds were chosen at $P < 0.05$ and $P < 0.01$, respectively.

Results

A. hydrophila and SVCV infection causes brief clinical symptoms

The viability of infected fish was evaluated, and several gross characteristics were seen at various time intervals following *A. hydrophila* challenge, including body

surface bleeding, anal inflammation, abdominal dropsy, and intestinal mucosal lesions in injected fish. *A. hydrophila* was found after re-isolating bacteria from fish internal organs (Di et al. 2017).

After SVCV challenge, the sick fish had usual clinical symptoms such as lack of appetite and sluggish behavior; over 80% of infected fish displayed characteristic ascites and edema at 2 dpi. Individuals with significant bleeding signs begin to die on day three, yet survivors show no symptoms and continue to swim normally seven days later. External lesions such as belly bloating exophthalmia, enlarged abdomen pale gills, loss of scales, and bleeding in the caudal fins and skin were also observed in the infected group. Throughout the investigation, the control group had none of these clinical indicators. Furthermore, a semi-nested PCR was used to amplify the SVCV glycoprotein gene, and the bands were obtained from tissue filtrates of sick fish, indicating that the virus could invade EPC cells and cause them to show obvious CPE. All of these demonstrated that the SVCV can successfully invaded tissue following intraperitoneal injection.

Molecular characterization of *Cc*Rab5A

The full-length cDNA sequences of *Cc*Rab5A were successfully acquired for this work using the RACE technique. The total length of the *Cc*Rab5A cDNA was 2434 base pairs, with the ORF accounting for 651 base pairs, the 3' UTR for 1064 base pairs, and the 5′ UTR for 719 base pairs (Fig. 1).

The domain of *Cc*Rab5A of Yellow River Carp was predicted by SMART online software. The results showed that *Cc*Rab5A contained a conservative Rab domain (22–185 amino acids) (Fig. 2A). TMHMM predicted the transmembrane structure of the protein (Fig. 2B), and the Yellow River Carp *Cc*Rab5A had no transmembrane structure. Through the prediction of signal peptide on SignalP website, it is concluded that the protein does not contain signal peptide and is a non-secretory protein. The 3D model of *Cc*Rab5A is constructed by Swiss-Model software, and the 3D model is analyzed by Swiss-Pdb Viewer 4.0.1 and PyMol software. The results were shown in Fig. 2C. Through the analysis and prediction of CBS-NetPhos 2.0 serverr website, 11 phosphorylation sites of the protein were identified, including 2 tyrosine (Tyr) phosphorylation sites, 1 threonine (Thr) phosphorylation site and 8 serine (Ser) phosphorylation sites (Fig. 2D). The Yellow River Carp *Cc*Rab5A is composed of multiple irregular curls and 6 β-Fold and 4 α-Spiral composition. Through online software http://www.csbio.sjtu.edu.cn/bioinf/Cell-PLoc-2/. The subcellular localization of *Cc*Rab5A was predicted. The prediction results showed that *Cc*Rab5A was mainly localized on the cell membrane and various endosomes.

Spatial structures of *Cc*Rab5A

The spatial structures of *Cc*Rab5A were predicted using Swiss-model software and the internet program PSIPRED. According to the findings, *Cc*Rab5A's secondary structures featured four -helices and six -strands, which was in line with the structural characteristics of other Rab GTPases. The four helices and six strands structure were hypothesized to have a significant role in their function (Fig. 2C). Ras-related protein Rab-5A, having a sequence identity of 98.24%, the model 1tu3.1was used as the basis for the prediction of the spatial structure of *Cc*Rab5A (Fig. 2C).

```
1     GGGGGGGCGGAGCCTATGGAAAAACGCCAGCAACGCGGCCTTTTTACGGTTCCTGGCCTTTTGCTGGCCTTTTGC
76    TCACATGTTCTTTCCTGCGTTATCCCGTGATTCTGTGGATAACCGTATTACCGCTTTTGAGTGAGCTGATACCGC
151   TCGCCGCAGCCGAACGACCGAGCGCAGCGAGTCAGTGAGCGAGGAAGCGGAAGAGCGCCCAATACGCAAACCGCC
226   TCTCCCCGCGCGTTGGCCGATTCATTAATGCAGCTGGCACGACAGGTTTCCCGACTGGAAAGCGGGCAGTGAGCG
301   CAACGCAATTAATGTGAGTTAGCTCACTCATTAGGCACCCCAGGCTTTACACTTTATGCTTCCGGCTCGTATGTT
376   GTGTGGAATTGTGAGCGGATAACAATTTCACACAGGAAACAGCTATGACCATGATTACGCCAAGCTTGCATGCCT
451   GCAGGTCGACGATTGACTCGAGTCGACATCGATTTTTTTTTTTTTTTTTTTTTTTTTTTTGAGAAAAGAA
526   AGGAGGAGACTTGATCGGGGTTGGTAAAATTCCCACTAACTGACCCCAATAAGAAGGAAAACCTCTAGAAAATTT
601   GAGCACTCCGTCGTCGGAAATCAGTTTCCGCAACCTGTCGGCTGACATTCAGCCAGTACTGGGACAGCTCTCAGT
676   GTGTGTGTGACCACTTAAAGGAGACGGGGTGATTGACGACTGCCATGGCCAATAGGGGAGGAGCAACACGCCCCA
1                                                     M  A  N  R  G  G  A  T  R  P
751   ACGGGTCCAACGCGGGCAATAAGATCTGCCAGTTTAAACTGGTGTTGTTAGGAGAATCAGCTGTGGGAAAGTCCA
11    N  G  S  N  A  G  N  K  I  C  Q  F  K  L  V  L  L  G  E  S  A  V  G  K  S
826   GCCTCGTACTGCGCTTCGTCAAGGGGCAGTTTCATGAGTTTCAGGAAAGCACAATAGGAGCGGCCTTCCTTGCAC
36    S  L  V  L  R  F  V  K  G  Q  F  H  E  F  Q  E  S  T  I  G  A  A  F  L  A
901   AGACGGTGTGCTTAGATGACACAACGGTAAAGTTTGAGATTTGGGACACAGCCGGACAGGAGCGCTACCACAGTT
61    Q  T  V  C  L  D  D  T  T  V  K  F  E  I  W  D  T  A  G  Q  E  R  Y  H  S
976   TGGCCCCCATGTACTATAGAGGTGCCCAGGCTGCCATTGTAGTTTATGACATCACCAATGAGGAGTCGTTTGCAA
86    L  A  P  M  Y  Y  R  G  A  Q  A  A  I  V  V  Y  D  I  T  N  E  E  S  F  A
1051  GAGCAAAGAACTGGGTTAAGGAGCTTCAGAGGCAGGCCAGTCCAAATATTGTCATCGCACTGTCTGGGAACAAGG
111   R  A  K  N  W  V  K  E  L  Q  R  Q  A  S  P  N  I  V  I  A  L  S  G  N  K
1126  CTGACCTTGCCAACAAGAGAGCTGTGGACTTCCAGGATGCTCAGTCTTATGCAGACGACAACAGTTTGTTGTTCA
136   A  D  L  A  N  K  R  A  V  D  F  Q  D  A  Q  S  Y  A  D  D  N  S  L  L  F
1201  TGGAGACGTCAGCAAAGACTTCCATGAATGTCAATGAGATCTTCATGGCCATTGCGAAAAGGTTGCCTAAGAATG
161   M  E  T  S  A  K  T  S  M  N  V  N  E  I  F  M  A  I  A  K  R  L  P  K  N
1276  AGCCCCAAGCCGCCGGAGCCAGCAGTGGGCGGAGTAGGGGCGTGGACCTCACAGAGACAGCCCAACCCACTAAGG
186   E  P  Q  A  A  G  A  S  S  G  R  S  R  G  V  D  L  T  E  T  A  Q  P  T  K
1351  CCCCCTGCTGCAGCAACTAACGCAAAACAAATCCCCCTCCACCAAACTCTGTTACCGCGACAACTAACGCAAGGT
211   A  P  C  C  S  N  *
1426  CCCGCCCTCCAACTTGGTTTTTGACTAACTAATGAAATGCGTCCGCTTTCCCCATTTTCCACAACTCTCTTACGC
1501  TGTAACAAAAGCTCTGCCCCGACCATGTAGCTACAGTGTTCTTGTTTTGTTGTTTTTCTGTAAAGACCCAGGCCT
1576  CTTACTGTATTCATGCTTAAGTTCATGCCGTGTCTCCGAATTGTAATATATGCCGTCACAGATATCCATCAAAAA
1651  AAAAAAAAAAATCTAAATTCCTTTTGCCTGACCTGGACAAAAGGGGTGGGGCCTCTTCAAAGGTTCACCTGCCCT
1726  GTCATAATTGAAAACGCTTCTTTTTCCCAAATCTGTTTTCATCTTTTTTATGATTTAGTTTTATAAGAAATGTAC
1801  TTTTCCGAAATATGAAGCATGTATCACTACAAAGCCTGAAATGCTAAATCAGAGTTTAACCGTATACACCGTCAC
1876  ACATGGCGAAAGAGACGTGACGAGTACCCAGCCTGCTCACTCGTCCCCTGGTTCCTTTTTGGTCCTGCCTGGCTC
1951  GCCATTTGGTCTTGATTTTCCCTGGTCCTGGCCTTTGCTGTAGATTTTTTTTTCCATCCGTTGTCATTTAAGCGG
2026  TAGGTCGTTACTGAATAAGATTAACTCAGTCCATTTCAACTTTCCTCCGTGCTTCAGTTTTTTGGTGATATTTTT
```

Fig. 1 cDNA sequence and predicted amino acid sequence of Yellow River Carp *Cc*Rab5A. Note: Red colors represented PM domain, blue colors represented G domain, green colors represented RabF domain; "*" indicates the stop codon

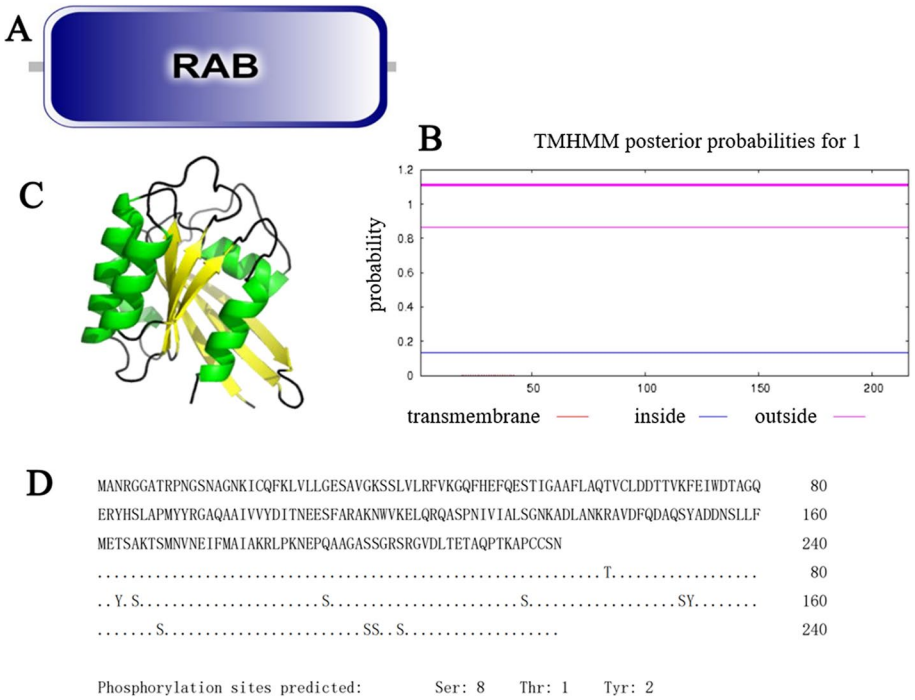

Fig. 2 **A**. Schematic diagram of the domain of Yellow River Carp *Cc*Rab5A. **B**. Prediction of *Cc*Rab5A transmembrane domain. **C** The three-dimensional structure of CRD in the *Cc*Rab5A.Note: The α-helices, β-sheets, and coils are shown in green, yellow and black. **D**. Phosphorylation sites of Yellow River Carp RAB5A

Phylogenetic analysis and molecular variants

The RAB domain and low complexity of the deduced amino acid sequences of CcRab5A (Fig. 2A) showed high identity to those of *Cyprinus carpio* (99.54%), *Onychostoma macrolepis* (98.61%), *Sinocyclocheilus grahami* (98.15%), *Mastacembelus armatus* (97.22%) and *Danionella translucida* (96.76%) (Table 2). According to the Amino acid alignment sequence analysis, the identified *Cc*Rab5A contained the conserved guanine-base binding motifs (G) and phosphate/magnesium-binding motifs (PM).

Guanine-base binding motifs (G), phosphate/magnesium-binding motifs (PM), Rab family (RabF) motifs, as well as the mutable N and C terminals, have some common structural characteristics. The multiple alignments of the amino acid sequence revealed the prototypical PM motif sequences of *Cc*Rab5A in various species to be "GESAVGKS (28–35)", "F (46)", and "DTAGQE (76–81)" (Red boxes), while the prototypical G motif sequences to be "T (53)", "NKADL (134–138)", and "SAK (164–166)" (Blue boxes). *Cc*Rab5A was found to have Rab-conserved sequences, commonly known as Rab family (RabF) motifs. They were "IGAAF (54–59)", "KFEIW (71–75")", "RYHSLA (82–87")", "YYRG (90–93)", and "VVYDIT (99–104")" (green boxes). At the C terminal of *Cc*Rab5A, the double-cysteine prenylation motif "CCSN" was also discovered and was conserved across multiple species (Fig. 3).

Table 2 The similarity and identity between *Cc*Rab5A and Rab5s from other species

Species	GenBank accession	Similarity (%)	Identity (%)
Cyprinus carpio	XP_018938893.1	99.54	99.54
Danio rerio	AAI65915.1	96.30	94.44
Onychostoma macrolepis	XP_016303800.1	99.07	98.61
Sinocyclocheilus grahami	XP_016136858.1	98.61	98.15
Danionella translucida	TRY74159.1	98.15	96.76
Mastacembelus armatus	XP_026155826.1	98.61	97.22
Oreochromis niloticus	XP_003443197.1	97.22	93.00
Oncorhynchus kisutch	XP_031651067.1	98.61	96.30
Lepisosteus oculatus	XP_015212924.1	97.69	94.44
Salmo trutta	XP_029595012.1	95.37	91.67
Homo sapiens	CAG38731.1	21.30	8.80
Mus musculus	BAF02855.1	20.83	8.80

Using MEGA 8.0's neighbor-joining approach and the *Cc*Rab5A sequences from different species, a phylogenetic connection was created (Fig. 4). The findings revealed that whereas amphibians, birds, fish, and mammals fell into one large group, invertebrates were grouped into a separate group.*Cc*Rab5A gene expression in various *C. carpio* tissues.

The recombinant protein and polyclonal antibody of *Cc*Rab5A

E. coli BL21 (DE3)-pLysS was created by transforming the recombinant plasmid (pET-32a-*Cc*Rab5A). The whole cell lysate of *E. coli* BL21 (DE3)-pLysS with pET-32a-CcRab5A was examined by SDS-PAGE following IPTG induction. 43 kDa was the molecular weight of a distinct band that was seen. A polyclonal antibody was made using the purified *Cc*Rab5A protein, and western blotting was utilized to determine the specificity of the antibody against *Cc*Rab5. The presence of a single, distinct band with a molecular weight identical to *Cc*Rab5A demonstrated the great specificity and effectiveness of the polyclonal antibodies (Fig. 5).

Differential expression of *Cc*Rab5A in different tissues

Total RNA was extracted from 11 different tissues of unchallenged Yellow River Carp. The tissue distribution of *Cc*Rab5A transcripts were analyzed using the qRT-PCR method. β-actin was used as the loading control. Assays were performed three times, and data are presented as means ± SD of three independent assays. The mRNA transcripts of *Cc*Rab5A could be detected in all tested tissues including head kidney, bood, heart, liver, muscle, brain, gill, skin, spleen, intestine, and kidney. According to the results of real-time PCR (Fig. 6A), the results showed that the expression of *Cc*Rab5A was the highest in head kidney, higher in blood tissue while the expression level of *Cc*Rab5A was very low in skin, spleen, intestine and kidney.

After extracting total protein from four tissues (liver, muscle, intestine and spleen) of the Yellow River Carp, SDS-PAGE electrophoresis, membrane transfer, incubation of the first antibody, incubation of the second antibody and ECL luminescence detection were

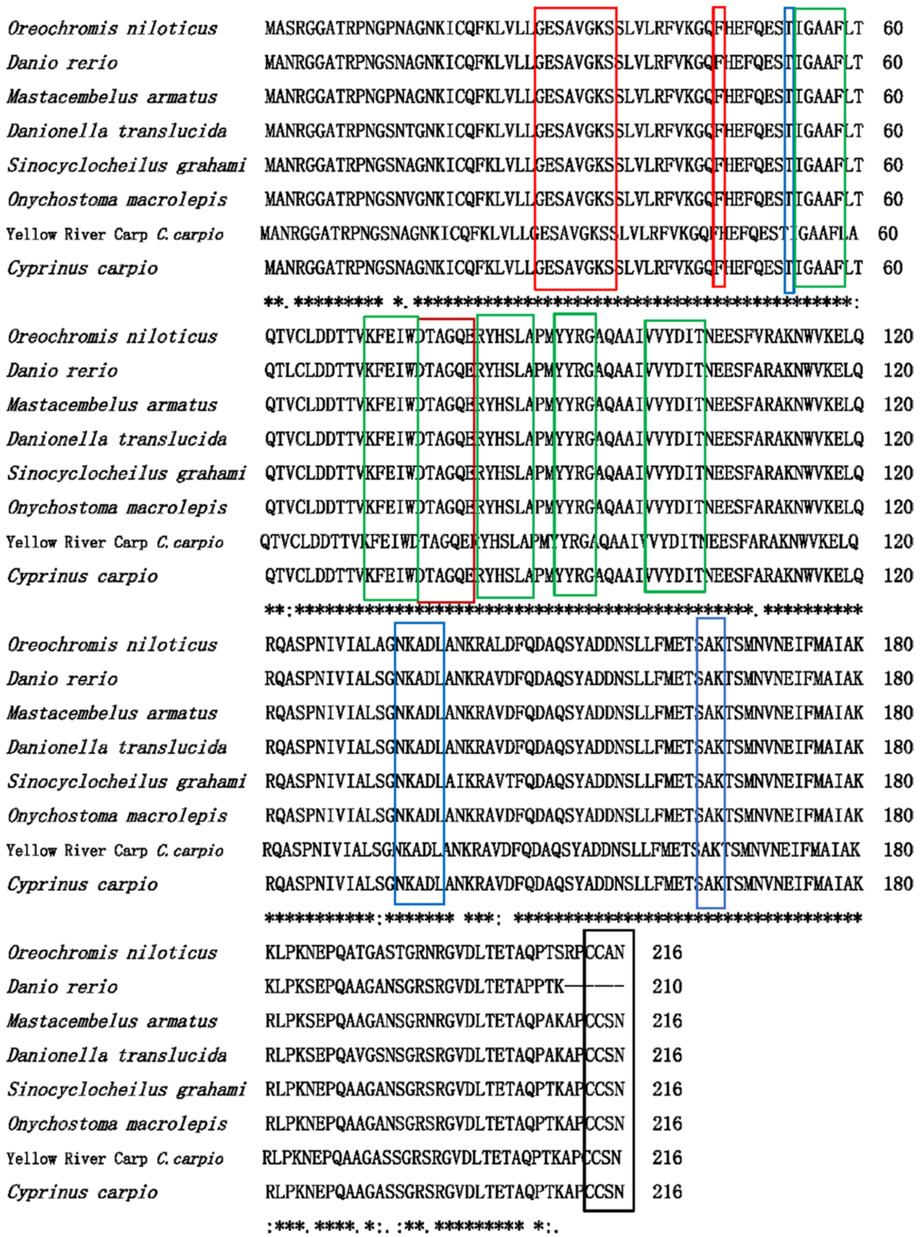

Fig. 3 Sequence alignment of *Cc*Rab5A A full-length amino acids between Yellow River Carp and other fishes. Note: Red boxes indicate PM domain, blue boxes indicate G domain and green boxes indicate RabF domain

performed. The results showed that the *Cc*Rab5A protein of the Yellow River Carp had different expression in different tissues (Fig. 6B), the results showed that the account of *Cc*Rab5A protein shared essentially similar as amount of mRNA.

Fig. 4 Neighbour-joining phylogenetic tree of of *Cc*Rab5A amino acid sequences from different species. with MEGA7.0 software. Note: Accession numbers of amino acids sequences used for phylogenic analysis are *Mus musculus* (AB232593.1), *Larimichthys crocea* (KP676384.1), *Homo sapiens* (CR536492. 1), *Danio rerio* (NM_200970.1), *Rattus norvegicus* (NM_022692.1), *Macaca fascicularis* (NM_001283973.1), *Petunia hybrida* (MH986793.1), *Oryza sativa* (AJ292320.1), *Cyprinus carpio* (XM_019083348.1), *Sinocyclocheilus rhinocerous* (XM_016563611.1), *Astyanax mexicanus* (XM_022662979.1), *Oncorhynchus kisutch* (XM_020507850.2), *Salmo trutta* (XM_029739152.1), *Salvelinus alpinus* (XM_023980144.1), *Salmo salar* (NM_001140145.1), *Ictalurus punctatus* (NM_001200567.1), *Xiphophorus hellerii* (XM_032580074.1), *Sparus aurata* (XM_030394584.1), *Oncorhynchus nerka* (XM_029625924.1), *Cottoperca gobio* (XM_029451770.1), *Haplochromis burtoni* (XM_005923726.1)

Temporal expression patterns of *Cc*Rab5A after SVCV and *A. hydrophila* challenges

To investigate the role of *Cc*Rab5A gene, SVCV and *A. hydrophila* challenge experiments were performed. The expression of *Cc*Rab5A were profiled in liver, skin,intestine, gill and spleen by qRT-PCR after carp were infected with SVCV and *A. hydrophila*, respectively. the transcriptional levels of *Cc*Rab5A increased in intestine after SVCV infection at 12 hpi ($p < 0.01$). Compared with the control group, the transcriptional levels of *Cc*Rab5A in SVCV stimulation group also began to decrease at 6 hpi ($P < 0.05$), but reached the peak

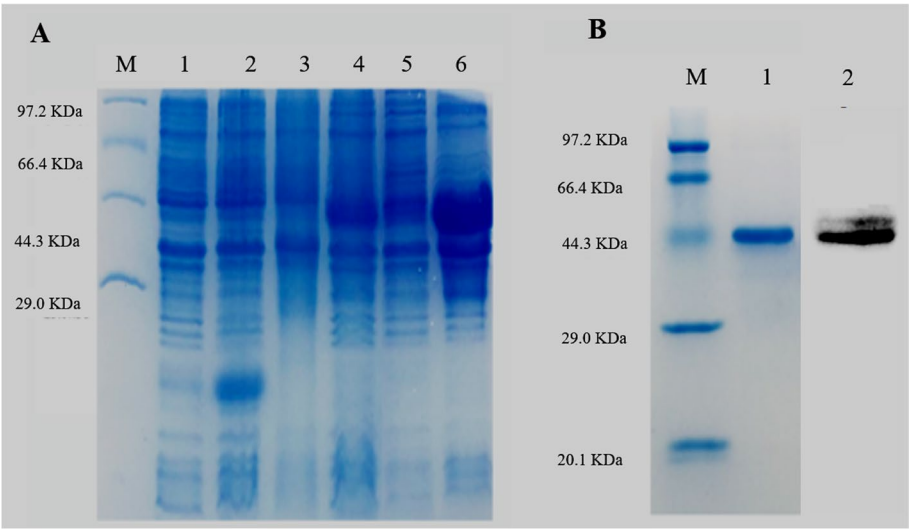

Fig. 5 SDS-PAGE and western blotting confirm the expression of recombinant proteins and the specificity of mouse anti-*Cc*Rab5A. Note: **A** Expression of *Cc*Rab5A recombinant protein; **B** specificity of recombinant protein polyclonal antibody detected by western blot. M, protein Maker; **A** lane 1, 32a is not induced without load; lane 2, 32a no-load induction; lane 3, *Cc*Rab5A was not induced; lane 4, *Cc*Rab5A induction; lane 5, *Cc*Rab5A ultradisrupted supernatant; lane 6, *Cc*Rab5A ultra-broken precipitate. **B** lane 1. purification of *Cc*Rab5A protein; lane 2. Western blot results of specific binding between *Cc*Rab5A polyclonal antibody and recombinant protein

at 12 hpi, which was 1.9 times that in the control group ($P < 0.01$), and then decreased at 24, 48 and 72 hpi, it returned to normal level slowly, but there was no significant change compared with the control group ($P > 0.05$). In liver, the transcriptional levels of *Cc*Rab5A also increased at 6 h after SVCV infection ($P < 0.05$), but reached the peak at 48 h, which was 4.3 times that in the control group, the expression showed a very significant difference ($P < 0.01$), and then decreased gradually at 72 h, but it was still significantly higher than that in the control group ($P < 0.01$). In gill, the transcriptional level of *Cc*Rab5A was up-regulated at 6 h, 12 h and 48 h, and the up-regulation range was the highest at 6 h after SVCV infection ($P < 0.01$), which was 9 times that of the control group. Compared with the control group, the transcriptional level of *Cc*Rab5A was very significant ($P < 0.01$), Then the transcriptional levels of *Cc*Rab5A slowly returned to normal at 72 h. In skin, the expression was up-regulated at 12 h and 48 h, and down regulated at 6 h after SVCV infection, which was significantly different from that in the control group ($P < 0.01$). In spleen, the expression trend of *Cc*Rab5A increased slightly at 12 h after SVCV infection ($P < 0.05$) (Fig. 7).

Upon *A. hydrophila* infection, in the liver, the transcriptional levels of *Cc*Rab5A increased at 6 h ($P < 0.05$) and 12 h, 24 h after treatment, the transcriptional level of *Cc*Rab5A was significantly decreased at 24 h ($P < 0.05$); Then it increased slowly and returned to normal level at 72 h. In the intestine, the transcriptional levels of *Cc*Rab5A was significantly lower than that of the control group at 6 h ($P < 0.05$); Then the transcriptional levels of *Cc*Rab5A began to increase gradually, and showed a very significant difference at 12 h and 48 h ($P < 0.01$). It reached the peak at 48 h, which was three times that of the control group; At 72 h, the transcriptional levels of *Cc*Rab5A decreased slightly, but there was still significant up-regulated ($P < 0.05$). In gills, the transcriptional levels of

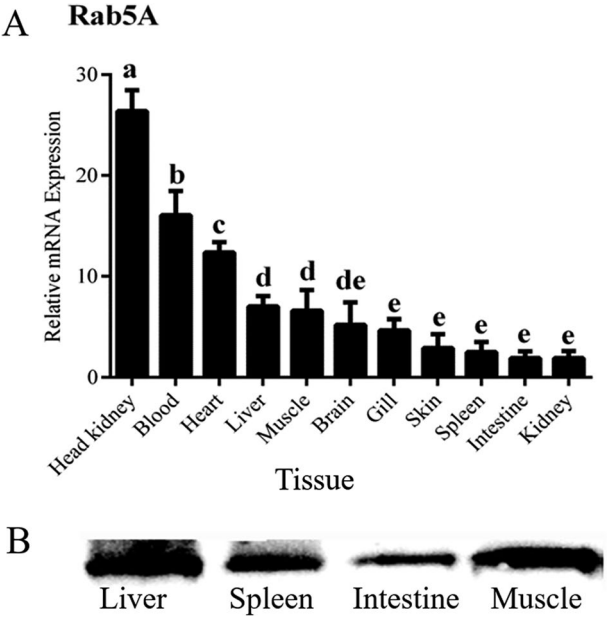

Fig. 6 The expressions of *Cc*Rab5A in different tissues of Yellow River Carp. **A** The expressions of *Cc*Rab5A at mRNA level in different tissues; **B** Tissue specificity of *Cc*Rab5A protein expression by Western blot. Note: Three Yellow River Carps were chosen to eliminate individual differences. β-actin served as the loading control. Error bars represent the mean ± S.D of three independent assays. The expression lever of *Cc*Rab5A in different tissues of Yellow River Carp; the expression level in kidney was set as 1, and that in other tissues is multiple of that in kidney; Vertical bars represent the mean ± S.D. ($N = 3$). The same letters above bars indicate that expression levels were not significantly different, while different letters indicate significant differences ($P < 0.05$)

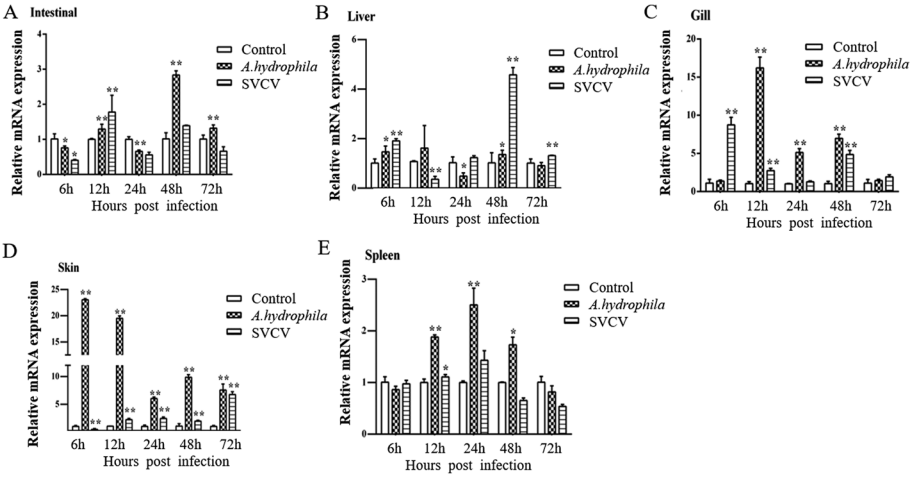

Fig. 7 Temporal expression patterns of *Cc*Rab5A in five tissues of Yellow River Carp after infection with *A.hydrophila* and SVCV. Note: **A** Intestinal tracty, **B** Liver, **C** Gill, **D** Skin, **E** Spleen. The expression level of control group was set as 1, Values were shown as mean ± SD ($n = 3$). "*" indicates significant difference ($p < 0.05$), "**" indicates that the difference was extremely significant ($p < 0.01$)

*Cc*Rab5A began to increase, and showed a very significant difference at 12 h, 24 h and 48 h ($P < 0.01$). It reached the peak at 12 h, which was 17 times that of the control group. In the skin, the transcriptional levels of *Cc*Rab5A were up-regulated at 6, 12, 24,48,72 h ($P < 0.01$). The up-regulation range was the highest at 6 h, which was 23 times that of the control group. In the spleen, the transcriptional levels of *Cc*Rab5A increased at 12 h and 24 h, reached the peak at 24 h ($P < 0.01$). The expression began to decrease at 48 h and 72 h, and showed a trend of increasing. first and then decreasing (Fig. 7).

Subcellular localization of *Cc*Rab5A in Yellow River Carp

The recombinant plasmid N3-Rab5A was digested with EcoR I and Hind III, and the products were detected by electrophoresis. The results are shown in Fig. 8. The digested products have two bright bands consistent with the theoretical value in the same lane, indicating that the recombinant plasmid has been successfully constructed.

In order to investigate the localization of *Cc*Rab5A in cells, the project constructed a recombinant expression vector and transfected it into GCO cells. The experimental results (as shown in Fig. 9) showed that the recombinant expression vector *Cc*Rab5A in GCO cells was pan-cellular distributed in GCO cells, online software was used to predict the subcellular localization of *Cc*Rab5A. The results showed that *Cc*Rab5A was mainly localized on the cell membrane, nucleus and various endosomes, such as various vesicles, Golgi bodies and endoplasmic reticulum.

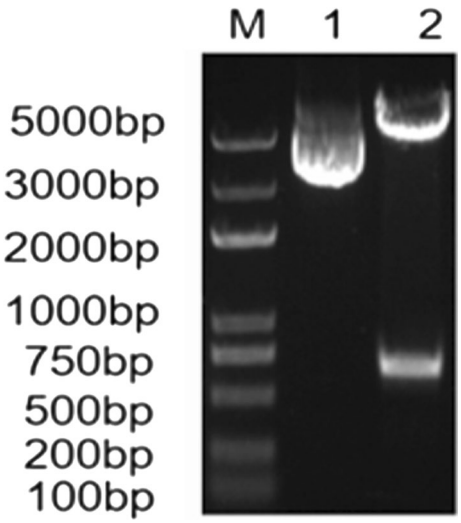

Fig. 8 Verification of recombinant plasmid by PCR double digestion. Note: (A) double digestion verification of recombinant plasmid N3-Rab5A; Lane M: DNA Marker; Lane 1: pEGFP-N3; Lane 2: N3-Rab5A double enzyme digestion product

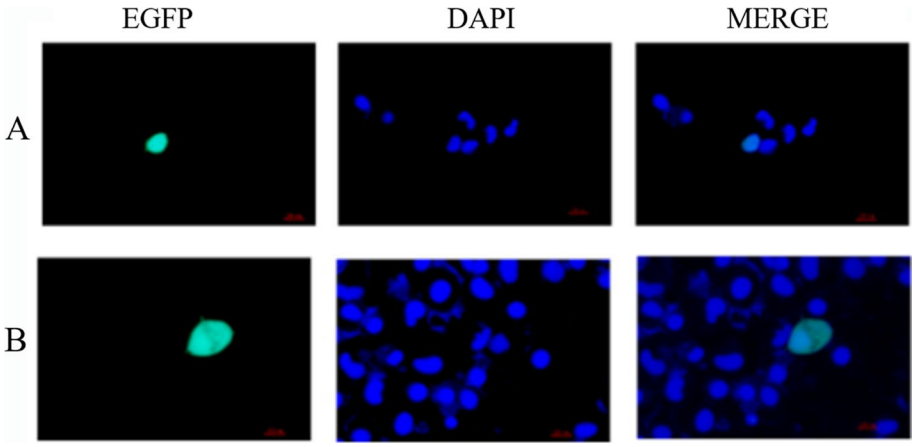

Fig. 9 Positioning of *Cc*Rab5A in GCO. Note: **A** is the empty vector pEGFP-N3, **B** is the recombinant vector of *Cc*Rab5A and pEGFP-N3; green fluorescence indicates the target gene, blue fluorescence is the nucleus, merge indicates fusion diagram of two fluorescences

Discussion

More than 70 Rab proteins have been identified from the human genome to date (Li and Marlin 2015). Rab GTPase is well known for its role in regulating intracellular membrane trafficking between organelles, particularly interactions between intracellular compartments and phagosomes (Schmitt et al. 1986; Flannagan et al. 2012; Bhuin and Roy 2014; Li and Marlin 2015). Rabs can interact with multiple effectors both temporally and spatially to facilitate cargo selection into vesicles, Vesicle anchoring to a target compartment and migration along actin and microtubule cables in preparation for membrane fusion (Yang et al. 2016). A particular Rab network was created by several Rab proteins in the Rab family, and it controls the complex connections between the phagosome and numerous intracellular compartments. They play an important role in immune processes, particularly the formation of endosomes, which influences endocytosis in both invertebrates and vertebrates (Brumell and Scidmore 2007). Rab proteins have long been recognized as important regulators of endocytic pathways (Takai et al. 2001; Yang et al. 2016). Rab GTPases have been linked to the infection of a variety of microbial pathogens (Wandinger-Ness and Zerial 2014).

Several Rab subfamily members, including Rab5, Rab7, Rab9, and Rab24, have been implicated in the intracellular replication of bacterial pathogens such as *Mycobacterium tuberculosis*, *Coxiella burnetii*, and *Salmonella enterica serovar* Typhimurium (Salcedo and Holden 2005; Brumell and Scidmore 2007). Rab5 molecules are central to this Rab network and have a significant impact on phagosome maturation (Vieira et al. 2003; Starr et al. 2010; Flannagan et al. 2012). Rab5 has cellular functions other than regulating intracellular membrane trafficking, such as signal transduction, autophagy, and phagocytosis (Li and Marlin 2015). Clathrin-coated vesicles and the fusion of coated vesicles with sorting vesicles have both been linked to Rab5 (Bucci et al. 1992). Rab5 has been linked to hepatitis C virus replication as well as dengue and West Nile virus entry into HeLa cells (Stone et al. 2007). Recent research has revealed that Rab5 is

also involved in the innate immune response in a variety of species, particularly invertebrates (Zong et al. 2008; Ye et al. 2012; Liu et al. 2018).

Except for the critical conserved G and PM motifs, Rab proteins and other small GTPases have little sequence similarities. While PM motifs were known as phosphate/magnesium-binding motifs, G motifs (G1-G3) were implicated in guanine binding (Valencia et al. 1991). In the Ras superfamily, two conserved structural regions—the G motif and the PM motif—have been employed as distinguishing characteristics from other small GTPases. Within the Rab family, RabF motifs are conserved and distinct areas that could be exploited to recognize novel Rab proteins (Pereira-Leal and Seabra 2000). The conserved G, PM, and RabF motif areas of CcRab5A were discovered to be identical to those of other species (Fig. 4). The primary functional domains of Rab proteins were found to be substantially conserved across species, according to the research. Contrary to the conserved G, PM, and RabF domains, the N- and C-terminal portions of Rabs were revealed to be hypervariable in length and nucleotide sequence. High diversity in the N- and C-terminal areas is necessary for prenylation and targeting to certain intracellular membranes, claim by (Chavrier et al. 1991) and Steele-Mortimer et al. 1994). Double-cysteine prenylation motifs (two cysteine residues) found at the C-terminus of Rab proteins are linked to their reversible membrane localization. At the C-terminus of *Cc*Rab5A, several prenylation motifs (CCSN or CXXX) were identified in this work. Due to variations in prenylation patterns, *Cc*Rab5A may be distributed differentially in various internal membranes and organs.

The entire length of *Cc*Rab5A from Yellow River Carp *C. carpio* was successfully cloned in this study. *Cc*Rab5A is responsible for encoding 216 amino acids. The amino acid sequence analysis reveals that the *Cc*Rab5A protein has three main secondary structures: loop structure (LOOP), helix and fold (STRAND), and a simple RAB domain without transmembrane and signal peptide. GTP binding and hydrolysis regions are highly conserved, and the cysteine at the carboxyl end of GTP can be isoprene modified, which is essential in the process of cell membrane localization and promotes RAB protein-membrane binding. The amino acid sequence of *Cc*Rab5A protein G1 was T, G2 was GNKAD, and G3 was SAK; the amino acid sequence of PM1 was GESAVGK, PM2 was F, and PM3 was DTAGQE; and the amino acid sequence of Rab F1 was IGAAF, RYHSL, YYRGA, and VYDIT. The molecular switch region is the region of GTP-GDP binding and hydrolysis in the G domain; the PM region is the binding site of Mg2+ and phosphate, which is related to cell growth, migration, and protein transport; The Rab F region is the RAB protein's signature sequence, and it aggregates molecular switches Switch I and Switch II, which can change the conformation of GTP and GDP. The C-terminal amino acid is CCSN with a CXXX pattern, indicating that the Yellow River Carp *Cc*Rab5A protein can aid in the transport of early vesicles in cells during pathogen invasion, as well as sort and transport membrane components.

The Yellow River Carp *Cc*Rab5A protein has 11 phosphorylation sites; phosphorylation is related to kinase phosphorylation (Ashraf et al. 2016). Protein phosphorylation is the most fundamental, common, and important function for controlling protein activity and function, as well as the fundamental mechanism of cell signal transduction (Stenmark 2009). To carry out signal transduction, the Rab5A protein combines GDP/GTP with its own active GTP enzyme and converts between these two forms. The rapid translocation between the cytoplasm and the cell membrane regulates vesicle transport in the organism. Rab5A protein can participate in the maturation of lysosomes and phagosomes via self-phosphorylation and dephosphorylation, improve innate immune cell phagocytosis to pathogens, accelerate immune cell phagocytosis to pathogens,

and degrade exogenous antigens in lysosomes in anti-infection immunity (Cremers et al. 1994; Grosshans et al. 2006).

The *Cc*Rab5A protein of the Yellow River Carp was discovered to be a highly conserved protein through an amino acid sequence comparison of Cluster W. The similarity and consistency between the Yellow River Carp *Cc*Rab5A protein and the carp Rab5A (XP 018938893.1) protein was 99.54%, and the amino acid sequence of the Yellow River Carp was also highly similar to that of other fish. It is also very similar to other mammals and invertebrates, which supports the findings of this study, indicating the high stability and importance of this protein's function. A phylogenetic tree was built using the sequence of the Yellow River Carp's *Cc*Rab5A open reading frame. A branch was formed by all cyprinidae fish, *Sinocyclocheilus rhinocerous* (including the Yellow River Carp *Cc*Rab5A). The Yellow River Carp *Cc*Rab5A was found to be the most closely related to the carp Rab5A (XM 019083348.1) in the phylogenetic tree, which was consistent with the results of homology analysis.

Some Rabs are expressed in various human tissues, while others are tissue-specific (Stenmark and Olkkonen 2001; Gutierrez 2013; Li and Marlin 2015). Once the Rab GTPases were discovered at the cytosolic face of a separate membrane compartment, the biology of the compartment was subsequently defined (Gutierrez 2013; Li and Marlin 2015). *Cc*Rab5A was found in various tissues of *C. carpio* in this study, with the highest levels of expression found in the head kidney and blood. Vertebrate blood cells play critical roles in host humoral and cellular immunity, including recognition, encapsulation, phagocytosis, cytotoxicity mediation, nodule formation, and cell–cell communication. The high expression of *Cc*Rab5A in the head, kidney, and blood may indicate that *Cc*Rab5A was involved in *C. carpio*'s innate immunity. Two genes' expression levels were also relatively high in the heat and liver.

The amount of the gene expressed in different tissues reflects its important role in innate immunity. *Cc*Rab5A is widely expressed in 11 tissues of Yellow River Carp, with the highest levels in the head kidney, followed by blood, liver, and gills, which is consistent with the expression of large yellow croaker *Larimichthys crocea* (Zhang 2016) and shrimp (Wu et al. 2008). *Cc*Rab5A was found to be highly expressed in two immune-related organs, the head kidney and the blood, *Cc*Rab5A was found to be involved in the innate immune process of Yellow River Carp. Rab5A is a membrane protein that can be widely distributed on the surface of cell membranes (Barbieri et al. 2000), regulates the formation and maturation of early endosomes, is important in cell endocytosis (Lanzetti et al. 2004), and can transmit information and assist in molecular transport. There are a lot of macrophages in the head kidney and a lot of lymphocytes in the blood. When the fish body is stimulated, immune organs such as the head kidney, blood, and liver, as well as mucosal lymphatic immune organs, can rapidly up-regulate some immune genes, improving the body's immune defense. When Rab5A expression is inhibited, immune regulation becomes imbalanced, macrophage transportation is limited, cell endocytosis is uncontrollable, the ability to eliminate pathogens is weakened (Zhu et al. 2009), and synergistic immune stagnation occurs. Endocytosis was used for virus infection by mediating virus internalization or transporting virus particles to the site of replication (Seto et al. 2002; Sieczkarski and Whittaker 2002).

Spring viremia of carp is a major environmental and economic concern that affects cyprinids, primarily common carp (*Cyprinus carpio*), and has resulted in the most widespread disease and mass mortalities. Spring viremia of carp virus (SVCV), a member of the Rhabdoviridae family and the genus Vesiculovirus, is the causative agent of this disease. Infection with SVCV is highly lethal in young fish, with mortality rates of up to 90% (Baudouy et al. 1980), causing significant economic losses to the aquaculture industry. The disease is currently

endemic in Europe, North America, and a number of Asian countries, causing significant morbidity and mortality in affected fish. The problem presently has no workable solutions. When a virus infects a cell, the infectious nucleocapsid passes through the cell membrane and enters the cytoplasm. As a key player in organizing and maintaining the dynamic changes of the cell's inner membrane, Rab protein is involved in many cell processes, including vesicle formation and transportation (Lee et al. 2009).

The relative mRNA level of *Cc*Rab5A in the gill and intestine in this investigation after SVCV infection was comparable and indicates 12–48 h after injection. This outcome was consistent with the earlier discovery that *Litopenaeus vannamei*'s relative expression of Rab5 exhibited a pattern of decreasing initially before rising in response to WSSV and infection with the hypodermal and hematopoietic necrosis virus (IHHNV) (Zhao et al. 2015). The expression pattern was similar after virus analog treatment to large yellow croaker (Zhang 2016) and WSSV virus stimulation to shrimp (Nordmann et al. 2010). The nonstructural protein NS1 of IHHNV may also interact with Rab5 (Liu et al. 2018). In addition to being involved in the trafficking and infection of YHV in *Penaeus monodon*, Rab5 has also been found to interact with the NS1 protein of IHHNV (Liu et al. 2018; Posiri et al. 2016). Yellow head virus (YHV) infection and trafficking via Rab5 were both discovered in *Penaeus monodon* (Posiri et al. 2016). As a result, it was proposed that *Cc*Rab5A could aid virus entry and play an important role in WSSV infection. When these findings were combined, the result suggested that *Cc*Rab5A was related to *C. carpio*'s immune activity against WSSV infection.

The transcriptional level of *Cc*Rab5A was highly expressed in five tissues in the *A. hydrophila* treatment group. *Cc*Rab5A mRNA expression was reduced in the liver, gills, and intestine 6 and 24 h after *A. hydrophila* infection. After bacterial infection, *Cc*Rab5A transcriptional levels increased in the gill. Rab5A was significantly induced after *Vibrio parahaemolyticus* infection in large yellow croaker (*Larimichthys crocea*), and Rab5 could improve the inflammatory response of *L. crocea* (Han et al. 2017). In this study, the induced *Cc*Rab5A was linked to *C. carpio*'s nonspecific immune response to bacterial infection. *C. carpio* mRNA expression of *Cc*Rab5A was significantly induced by *A. hydrophila* infection. *Cc*Rab5A may participate in the immune response of Yellow River Carp stimulated by pathogens and play an important immune function, as demonstrated above. Gene expression patterns in *C. carpio*'s main immune tissues were determined after pathogen challenge to investigate the immune responses of *Cc*Rab5A to SVCV and *A. hydrophila*. The findings revealed that after pathogen infection, the transcriptional levels of *Cc*Rab5A fluctuated in different tissues in a time-dependent manner. After SVCV challenge, the liver and gills showed the greatest transcriptional level response.

Genes not only play an important role in innate immunity at the molecular level, but their protein expression can also reflect innate immunity. The proteins expression profiles of *Cc*Rab5A in 6 tissues were detected in this study, which are consistent with the expression at the mRNA level, this result is also consistent with that found in shrimp (Wu et al. 2008).

Conclusions

The full-length cDNA sequences of Rab5A from Yellow River Carp *C. carpio*, designed as *Cc*Rab5A, were successfully cloned in this study. *Cc*Rab5A has the classic structural features of the Rab GTPases protein family, which include highly conserved G, PM, and RabF motifs. *Cc*Rab5A was found in all tissues studied in *C. carpio*, with the highest levels found in the head, kidney, and blood. *Cc*Rab5A gene expression levels in *C. carpio*

Intestinal tracty, Liver, Gill, Skin, and Spleen were induced by SVCV and *A. hydrophila* infection. The digestive tract, liver, gills, skin, and spleen are all affected. *Cc*Rab5A was implicated in the innate immune response against WSSV infection in *C. carpio* in this study. The current data provide a theoretical foundation for further investigation into the immune functions of Rab5A in *C. carpio*.

Author contributions All the authors contributed to the study conception and design. Material preparation, data collection, methodology and analysis, Guilan Di and Ning Wang; conceptualization, methodology, and writing, Zeyuan Ma, Mingmei Jiang and Yu Zhang; funding acquisition, supervision, reviewing, and editing, Xinhua Chen and Guilan Di. All authors have read and agreed to the published version of the manuscript.

Funding This work was supported by the grants from the National Natural Science Foundation of China (U1905204), and the China Agriculture Research System of MOF and MARA (CARS-47), the Natural Science Foundation of Fujian Province of China (No. 2022J01586), Fuzhou Institute of Oceanography (2021F02).

Data availability Data are available on request due to privacy.

Declarations

Competing interests The authors declare that they have no known competing financial interests or personal relationships that could have appeared to influence the work reported in this paper.

References

Alvarez-Dominguez C, Barbieri AM, Berón W, Wandinger-Ness A, Stahl PD (1996) Phagocytosed live Listeria monocytogenes influences Rab5-regulated in vitro phagosome-endosome fusion. J Biol Chem 271(23):13834–13843. https://doi.org/10.1074/jbc.271.23.13834

Alvarez-Dominguez C, Stahl PD (1999) Increased expression of Rab5a correlates directly with accelerated maturation of Listeria monocytogenes phagosomes. J Biol Chem 274(17):11459–11462. https://doi.org/10.1074/jbc.274.17.11459

Ashraf U, Lu Y, Lin L, Yuan J, Wang M, Liu X (2016) Spring viraemia of carp virus: recent advances. J Gen Virol 97(5):1037–1051. https://doi.org/10.1099/jgv.0.000436

Barbieri MA, Roberts RL, Gumusboga A, Highfield H, Alvarez-Dominguez C, Wells A, Stahl PD (2000) Epidermal growth factor and membrane trafficking. EGF receptor activation of endocytosis requires Rab5a. J Cell Biol 151(3):539–550. https://doi.org/10.1083/jcb.151.3.539

Baudouy AM, Danton M, Merle G (1980) Virémie printanière de la carpe. Résultats de contaminations expérimentales effectuées au printemps [SVCV infection of Carp (author's transl)]. Annales de recherches veterinaires. Ann Vet Res 11(3):245–249.https://hal.science/hal-00901272

Baumgartner WA, Hawke JP, Bowles K, Varner PW, Hasson KW (2009) Primary diagnosis and surveillance of white spot syndrome virus in wild and farmed crawfish (*Procambarus clarkii*, *P. zonangulus*) in Louisiana, USA. Dis Aquat Org 85(1):15–22. https://doi.org/10.3354/dao02051

Bhuin T, Roy JK (2014) Rab proteins: the key regulators of intracellular vesicle transport. Exp Cell Res 328(1):1–19. https://doi.org/10.1016/j.yexcr.2014.07.027

Brumell JH, Scidmore MA (2007) Manipulation of Rab GTPase function by intracellular bacterial pathogens. Microbiol Mol Biol Rev 71:636–652. https://doi.org/10.1128/MMBR.00023-07

Bucci C, Lütcke A et al (1995) Co-operative regulation of endocytosis by three RAB5 isoforms. FEBS Lett 366(1):65–71. https://doi.org/10.1016/0014-5793(95)00477-Q

Bucci C, Parton RG, Mather IH, Stunnenberg H, Simons K, Hoflack B, Zerial M (1992) The small GTPase rab5 functions as a regulatory factor in the early endocytic pathway. Cell 70(5):715–728. https://doi.org/10.1016/0092-8674(92)90306-w

Chavrier P, Gorvel JP, Stelzer EH, Simons K, Gruenberg J, Zerial M (1991) Hypervariable C-termmal domain of rab proteins acts as a targeting signal. Nature 353:769–772. https://doi.org/10.1038/353769a0

Chen ZY, Liu H, Li ZQ, Wang M, Zhang QY (2006) Detection of viral pathogen from diseased common carp (*Cyprinus carpio*) by infectious tests. J Fish Sci China 13(4):617–623

Chen WC, Wang EL, Luo F, Song KG, Wang GX (2022) Identification and pathogenicity analysis of a novel highly virulent strain of spring viraemia of carp virus and production of its structural proteins by the mammalian expression system. Aquaculture 547. https://doi.org/10.1016/j.aquaculture.2021.737487

Cremers FP, Armstrong SA, Seabra MC, Brown MS, Goldstein JL (1994) REP-2, a Rab escort protein encoded by the choroideremia-like gene. J Biol Chem 269(3):2111–2117. https://doi.org/10.1016/S0021-9258(17)42142-9

Di G, Li H, Zhang C, Zhao Y, Zhou C, Naeem S et al (2017) Label-free proteomic analysis of intestinal mucosa proteins in common carp (*Cyprinus carpio*) infected with *Aeromonas hydrophila*. Fish Shellfish Immunol 66:11–25. https://doi.org/10.1016/j.fsi.2017.04.025

Flannagan RS, Jaumouillé V, Grinstein S (2012) The cell biology of phagocytosis. Annu Rev Pathol 7:61–98. https://doi.org/10.1146/annurev-pathol-011811-132445

Galea G, Bexiga MG, Panarella A, O'Neill ED, Simpson JC (2015) A high-content screening microscopy approach to dissect the role of Rab proteins in Golgi-to-ER retrograde trafficking. J Cell Sci 128(13):2339–2349. https://doi.org/10.1242/jcs.167973

Grosshans BL, Ortiz D, Novick P (2006) Rabs and their effectors: achieving specificity in membrane traffic. Proc Natl Acad Sci USA 103(32):11821–11827. https://doi.org/10.1073/pnas.0601617103

Gutierrez MG (2013) Functional role(s) of phagosomal Rab GTPases. Small GTPases 4(3):148–158. https://doi.org/10.4161/sgtp.25604

Han F, Song Q et al (2017) Molecular characterization and immune responses of Rab5 in large yellow croaker (Larimichthys crocea). Aquac Fish 2(4):165–172. https://doi.org/10.1016/j.aaf.2017.06.005

Hutagalung AH, Novick PJ (2011) Role of Rab GTPases in membrane traffic and cell physiology. Physiol Rev 91(1):119–149. https://doi.org/10.1152/physrev.00059.2009

Kim HJ (2012) Improved diagnosis of spring viremia of carp by nested reverse-transcription PCR: development of a chimeric positive control for prevention of false-positive diagnosis. J Virol Methods 185(1):39–42. https://doi.org/10.1016/j.jviromet.2012.05.027

Lanzetti L, Palamidessi A et al (2004) Rab5 is a signalling GTPase involved in actin remodelling by receptor tyrosine kinases. Nature 429(6989):309–314. https://doi.org/10.1038/nature02542

Lee MT, Mishra A, Lambright DG (2009) Structural mechanisms for regulation of membrane traffic by rab GTPases. Traffic (copenhagen, Denmark) 10(10):1377–1389. https://doi.org/10.1111/j.1600-0854.2009.00942.x

Li G, Marlin MC (2015) Rab family of GTPases. Methods Mol Biol (Clifton, NJ) 1298:1–15. https://doi.org/10.1007/978-1-4939-2569-8_1

Li C, Zhang Y, Yuan M, Zhu W, Pei C, Zhao X, Kong X (2023) An oral vaccine against spring viremia of carp virus induces protective immunity in common carp (*Cyprinus carpio* L.). Aquaculture 566:739167. https://doi.org/10.1016/j.aquaculture.2022.739167

Liu H, Jiravanichpaisal P, Cerenius L, Lee BL, Söderhäll I, Söderhäll K (2007) Phenoloxidase is an important component of the defense against Aeromonas hydrophila Infection in a crustacean, Pacifastacus leniusculus. J Biol Chem 282(46):33593–33598. https://doi.org/10.1074/jbc.M706113200

Liu Q, Li Q et al (2018) Interaction between Litopenaeus vannamei Rab5B protein (LvRab5B) and IHHNV proteins. J Fish China 42:1829–1839. https://doi.org/10.11964/jfc.20170810929

Liu J, Zhang P, Wang B, Lu Y, Li L, Li Y et al (2021) Evaluation of the effects of *Astragalus polysaccharides* as immunostimulants on the immune response of crucian carp and against SVCV in vitro and in vivo. Comparative biochemistry and physiology. Toxicol Pharmacol: CBP 253:109249

Lund VK, Madsen KL, Kjaerulff O (2018) Drosophila Rab2 controls endosome-lysosome fusion and LAMP delivery to late endosomes. Autophagy 14(9):1520–1542. https://doi.org/10.1080/15548627.2018.1458170

Mangkalanan S, Sanguanrat P, Utairangsri T, Sritunyalucksana K, Krittanai C (2014) Characterization of the circulating hemocytes in mud crab (Scylla olivacea) revealed phenoloxidase activity. Dev Comp Immunol 44(1):116–123. https://doi.org/10.1016/j.dci.2013.11.018

Murray JT, Panaretou C, Stenmark H, Miaczynska M, Backer JM (2002) Role of Rab5 in the recruitment of hVps34/p150 to the early endosome. Traffic (Copenhagen, Denmark) 3(6):416–427. https://doi.org/10.1034/j.1600-0854.2002.30605.x

Nordmann M, Cabrera M, Perz A, Bröcker C, Ostrowicz C, Engelbrecht-Vandré S, Ungermann C (2010) The Mon1-Ccz1 complex is the GEF of the late endosomal Rab7 homolog Ypt7. Curr Biol: CB 20(18):1654–1659. https://doi.org/10.1016/j.cub.2010.08.002

Pereira-Leal JB, Seabra MC (2000) The mammalian Rab family of small GTPases: definition of family and subfamily sequence motifs suggests a mechanism for functional specificity in the Ras superfamily. J Mol Biol 301(4):1077–1087. https://doi.org/10.1006/jmbi.2000.4010

Pereira-Leal JB, Seabra MC (2001) Evolution of the Rab family of small GTP-binding proteins. J Mol Biol 313(4):889–901. https://doi.org/10.1006/jmbi.2001.5072

Posiri P, Panyim S, Ongvarrasopone C (2016) Rab5, an early endosomal protein required for yellow head virus infection of Penaeus monodon. Aquaculture 459:43–53. https://doi.org/10.1016/J.AQUACULTURE.2016.03.026

Qiao D, Yan Y, Pei C, Zhang J, Zhao X, Jiang X, Zhu L, Zhang J, Li L, Kong X (2023) Characterization of hepcidin gene and protection of recombinant hepcidin supplemented in feed against *Aeromonas hydrophila* infection in Yellow River carp (*Cyprinus carpio haematopterus*). Fish Shellfish Immunol 139:108872. https://doi.org/10.1016/j.fsi.2023.108872

Qin Z, Sarath Babu V, Lin H, Dai Y, Kou H, Chen L, Li J, Zhao L, Lin L (2019) The immune function of prophenoloxidase from red swamp crayfish (Procambarus clarkii) in response to bacterial infection. Fish Shellfish Immunol 92:83–90. https://doi.org/10.1016/j.fsi.2019.05.005

Salcedo SP, Holden DW (2005) Bacterial interactions with the eukaryotic secretory pathway. Curr Opin Microbiol 8(1):92–98. https://doi.org/10.1016/j.mib.2004.12.007

Santos Y, Toranzo AE et al (1987) Relationships among virulence for fish, enterotoxigenicity, and phenotypic characteristics of motile Aeromonas. Aquaculture 67(1):29–39. https://doi.org/10.1016/0044-8486(87)90005-6

Schmitt HD, Wagner P et al (1986) The ras-related YPT1 gene product in yeast: A GTP-binding protein that might be involved in microtubule organization. Cell 47(3):401–412. https://doi.org/10.1016/0092-8674(86)90597-0

Seto ES, Bellen HJ, Lloyd TE (2002) When cell biology meets development: endocytic regulation of signaling pathways. Genes Dev 16(11):1314–1336. https://doi.org/10.1101/GAD.989602

Sieczkarski SB, Whittaker GR (2002) Dissecting virus entry via endocytosis. J Gen Virol 83(Pt 7):1535–1545. https://doi.org/10.1099/0022-1317-83-7-1535

Spaargaren M, Bos JL (1999) Rab5 induces Rac-independent lamellipodia formation and cell migration. Mol Biol Cell 10(10):3239–3250. https://doi.org/10.1091/mbc.10.10.3239

Starr T, Sun Y et al (2010) Rab33b and Rab6 are Functionally Overlapping Regulators of Golgi Homeostasis and Trafficking. Traffic 11(5):626–636. https://doi.org/10.1111/j.1600-0854.2010.01051.x

Steele-Mortimer O, Clague MJ, Huber LA, Chavrier P, Gruenberg J, Gorvel JP (1994) The N-terminal domain of a rab protein is involved in membrane-membrane recognition and/or fusion. EMBO J 13(1):34–41. https://doi.org/10.1002/j.1460-2075.1994.tb06232.x

Stenmark H, Olkkonen VM (2001) The Rab GTPase family. Genome Biol 2(5):REVIEWS3007. https://doi.org/10.1186/gb-2001-2-5-reviews3007

Stenmark H (2009) Rab GTPases as coordinators of vesicle traffic. Nat Rev Mol Cell Biol 10(8):513–525. https://doi.org/10.1038/nrm2728

Stone M, Jia S, Heo WD, Meyer T, Konan KV (2007) Participation of rab5, an early endosome protein, in hepatitis C virus RNA replication machinery. J Virol 81(9):4551–4563. https://doi.org/10.1128/JVI.01366-06

Takai Y, Sasaki T, Matozaki T (2001) Small GTP-binding proteins. Physiol Rev 81(1):153–208. https://doi.org/10.1152/physrev.2001.81.1.153

Valencia A, Chardin P et al (1991) The ras protein family: evolutionary tree and role of conserved amino acids. Biochemistry 30(19):4637–4648. https://doi.org/10.1021/bi00233a001

Vieira OV, Bucci C, Harrison RE, Trimble WS, Lanzetti L, Gruenberg J, Schreiber AD, Stahl PD, Grinstein S (2003) Modulation of Rab5 and Rab7 recruitment to phagosomes by phosphatidylinositol 3-kinase. Mol Cell Biol 23(7):2501–2514. https://doi.org/10.1128/MCB.23.7.2501-2514.2003

Wandinger-Ness A, Zerial M (2014) Rab proteins and the compartmentalization of the endosomal system. Cold Spring Harbor Perspect Biol 6(11):a022616. https://doi.org/10.1101/cshperspect.a022616

Wu W, Zong R, Xu J, Zhang X (2008) Antiviral phagocytosis is regulated by a novel Rab-dependent complex in shrimp penaeus japonicus. J Proteome Res 7(1):424–431. https://doi.org/10.1021/pr700639t

Yang XZ, Li XX, Zhang YJ, Rodriguez-Rodriguez L, Xiang MQ, Wang HY, Zheng XF (2016) Rab1 in cell signaling, cancer and other diseases. Oncogene 35(44):5699–5704. https://doi.org/10.1038/onc.2016.81

Ye T, Tang W et al (2012) Involvement of Rab6 in the regulation of phagocytosis against virus infection in invertebrates. J Proteome Res 11(10):4834–4846. https://doi.org/10.1021/pr300274k

Yu Z (2016) Molecular characterization and preliminary study of functions of Rab genes in *Larimichthys crocea* Master's thesis. Jimei University

Zhao YZ, Chen XL, Zeng DG, Yang CL, Peng M, Chen XH (2015) Molecular cloning, characterization, and expression of Rab5B, Rab6A, and Rab7 from Litopenaeus vannamei (Penaeidae). Genet Mol Res: GMR 14(3):7740–7750. https://doi.org/10.4238/2015.July.13.20

Zhu H, Liang Z, Li G (2009) Rabex-5 is a Rab22 effector and mediates a Rab22-Rab5 signaling cascade in endocytosis. Mol Biol Cell 20(22):4720–4729. https://doi.org/10.1091/mbc.E09-06-0453

Zong R, Wu W, Xu J, Zhang X (2008) Regulation of phagocytosis against bacterium by Rab GTPase in shrimp Marsupenaeus japonicus. Fish Shellfish Immunol 25(3):258–263. https://doi.org/10.1016/j.fsi.2008.05.006

Authors and Affiliations

Guilan Di[1,2] · Zeyuan Ma[1] · Mingmei Jiang[1] · Yu Zhang[1] · Ning Wang[2] · Xinhua Chen[1,3]

[1] State Key Laboratory of Mariculture Breeding, Key Laboratory of Marine Biotechnology of Fujian Province, Institute of Oceanology, College of Marine Sciences, Fujian Agriculture and Forestry University, Fuzhou 350002, China

[2] College of Fisheries, Henan Normal University, No. 46, Jianshe Road, Xinxiang 453007, China

[3] Laboratory for Marine Biology and Biotechnology, Qingdao National Laboratory for Marine Science and Technology, Qingdao 266071, China